

Entanglement of orbital angular momentum states between an ensemble of cold atoms and a photon

R. Inoue¹, N. Kanai¹, T. Yonehara¹,
Y. Miyamoto², M. Koashi³, M. Kozuma^{1,4,*}

¹Department of Physics, Tokyo Institute of Technology,

²Department of Information and Communication Engineering,
The University of Electro-Communications,

³ Division of Materials Physics, Graduate School of Engineering Science, Osaka University,

⁴ Japan Science and Technology Agency-PRESTO, CREST.

¹2-12-1 O-okayama, Meguro-ku, Tokyo 152-8550, Japan

²1-5-1 Chofugaoka, Chofu, Tokyo 182-8585, Japan

³1-3 Machikaneyama, Toyonaka, Osaka 560-8531, Japan

⁴1-9-9 Yaesu, Chuo-ku, Tokyo 103-0028, Japan

*E-mail: kozuma@ap.titech.ac.jp

Various atom-photon entangled states can be generated by utilizing corresponding conservation law. In particular, higher-dimensional entanglement between an atomic ensemble and a photon is expected to arise from angular momentum conservation law. Here we demonstrate entanglement of orbital angular momentum states by utilizing atomic collective excitation and Laguerre-Gaussian modes of light. Generation of higher-dimensional entanglement between remote atomic ensembles and an application to condensed matter physics are also discussed.

Higher-dimensional bipartite entangled states enable us to achieve more efficient quantum information processing (1, 2), for example by enhancing optical data traffic in quantum communications compared to usually employed two-dimensional entanglement between qubits. Such higher-dimensional entangled states can be created by using Laguerre-Gaussian (LG) modes, since photons in LG modes carry orbital angular momenta (OAM) which can be utilized to define an infinite-dimensional Hilbert space (3). Inspired by the pioneering experiment using parametric down-conversion (PDC) (4), various protocols have been demonstrated using the OAM states of photons (5, 6). However, PDC is a spontaneous process and the generation time of the entangled photons is completely random. Producing higher-dimensional entanglement between two remote long-lived massive atoms is therefore an important step toward the realization of intricate tasks of quantum information.

Recently, two-dimensional entanglement of a collective atomic excitation and a single photon has been successfully generated (7) using ‘DLCZ’ scheme (8). Two-dimensional entanglement of two remote atomic ensembles has also been reported (9, 10). In this Letter, we report entanglement of OAM states between a collective atomic excitation and a photon. While the measurement basis utilized in this study is limited to two dimensions, it is natural to presume that our system possesses higher-dimensional entanglement over a wide range of OAM.

Figure 1-A shows a schematic of our experimental setup. We consider ensemble of atoms having the level structure of $|a\rangle$, $|b\rangle$ and $|c\rangle$. Initially, all of the atoms are prepared in level $|a\rangle$. A classical *write* pulse tuned to the $|a\rangle \rightarrow |c\rangle$ transition with proper detuning Δ is emitted from a single mode fiber (SMF1) and is incident on the atomic ensemble. In this process, the $|c\rangle \rightarrow |b\rangle$ transition is induced and an anti-Stokes photon is generated. The *write* pulse is weak and its interaction time is short so that the probability of scattering one anti-Stokes photon into a specified mode is much less than unity for each pulse. We are interested in LG (LG_{0m}) modes

and a Gaussian (LG_{00}) mode. LG_{0m} modes have a doughnut-shape intensity distribution and carry corresponding OAM of $m\hbar$ per photon (3), which can be utilized to constitute an infinite-dimensional basis. Mode detection of the anti-Stokes photon is performed using a computer generated hologram (H1) and a single-mode fiber (SMF2). We can also analyze superpositions of an LG_{00} mode and an LG_{01} mode by shifting the dislocation of the hologram out of the center of the beam by a certain amount (11). Here we define $|m\rangle_{AS}$ to be the state of an anti-Stokes photon with OAM of $m\hbar$.

In the ideal case, detection of a single photon in a certain spatial mode results in the ensemble of atoms containing exactly one excitation in the corresponding collective atomic mode. The collective atomic spin excitation operator $\hat{S}^\dagger(\varphi)$ is given by

$$\hat{S}^\dagger(\varphi) \equiv \frac{1}{\sqrt{N}} \sum_j^N |b_j\rangle \langle a_j| e^{i\varphi(\mathbf{r}_j)}, \quad (1)$$

where the summation is taken over all the atoms and \mathbf{r}_j is the position of the j -th atom. $\varphi(\mathbf{r})$ corresponds to the spatial distribution of the relative phase between the *write* pulse and the detected anti-Stokes photon. The excited state of the atomic ensemble is given by $\hat{S}^\dagger(\varphi) |i\rangle_a$, where the initial state of the ensemble is $|i\rangle_a \equiv \otimes_j |a_j\rangle$. The atomic ensemble therefore memorizes the relative phase between the *write* pulse and the anti-Stokes photon. The write pulse has the mode profile of LG_{00} and propagates in the direction of wave vector \mathbf{k}_W , which is determined by SMF1. Here we only consider the anti-Stokes photon propagating in the direction of \mathbf{k}_{AS} determined by SMF2, which is almost the same as the direction of \mathbf{k}_W . Then, the relative phase $\varphi(\mathbf{r})$ is determined by the spatial mode profile of the detected anti-Stokes photon.

Suppose that the detected photon has the mode of LG_{0m} , and let $\varphi_m(\mathbf{r})$ be the relative phase in this case. The atomic ensemble is then in the excited state $| -m \rangle_a \equiv \hat{S}^\dagger(\varphi_m) |i\rangle_a$, which has the angular momentum with the opposite sign, $-m\hbar$, due to the angular momentum conservation law. The variation of $\varphi_m(\mathbf{r})$ along a closed path around the anti-Stokes beam

axis is $2m\pi$, implying that the atomic ensemble memorizes the phase structure of the emitted anti-Stokes photon including singularity.

If the detected anti-Stokes photon is in a mode which is a superposition of various angular momentum states, the state of the atomic ensemble becomes the corresponding superposition. This means that the whole state of the scattered anti-Stokes photon and the atomic ensemble is a coherent superposition of angular momentum states, which is written as

$$|\Psi\rangle_{\text{AS\&a}} = |\text{vac}\rangle_{\text{AS}} |i\rangle_a + \sqrt{p} \sum_{m=-\infty}^{\infty} C_m |m\rangle_{\text{AS}} | -m\rangle_a + \mathcal{O}(p), \quad (2)$$

where p and $|\text{vac}\rangle_{\text{AS}}$ represent the excitation probability and the vacuum state of the anti-Stokes photon. The amplitude C_m for each OAM state is expected to depend on the spatial shape of the region where the *write* pulse interacts with the atoms (12). Here, we consider the case of negligibly small $\mathcal{O}(p)$.

The entanglement shown in Eq.(2) can be verified as follows. After a variable delay δt , we convert the atomic excitation to a single photon (Stokes photon) by illuminating the atomic ensemble with a laser pulse (*read* pulse) resonant on the $|b\rangle \rightarrow |c\rangle$ transition. Note that the efficiency of this transfer can be very close to unity because it corresponds to the retrieval process based on electromagnetically induced transparency (13). Atom-photon entanglement, therefore, can be checked by measuring quantum correlation between the anti-Stokes and Stokes photons. Since we detect the Stokes photon counter-propagating with respect to the anti-Stokes photon, the value of the OAM of the Stokes photon in the direction of propagation is equal to that of the anti-Stokes photon. We use $|m\rangle_S$ to denote the state of a Stokes photon with OAM of $m\hbar$. In the present work, we investigated the entanglement concerned with $m = 0$ and $m = 1$.

In the experiment, we created an optically thick (optical depth ~ 4) cold atomic cloud using a magneto-optical trap (MOT) of ^{87}Rb . The levels $\{|a\rangle, |b\rangle\}$ correspond to $5S_{1/2}, F = \{2, 1\}$ levels, respectively, and the level $|c\rangle$ corresponds to $5P_{1/2}, F' = 2$. The experimental sequence

is shown in Fig.1-B schematically. One cycle of our experiment comprised of a cooling period and a measurement period, and both periods had durations of $500 \mu\text{s}$. After the cooling period, the magnetic field, the cooling and the repumping lights were turned off. The repumping light was left on for an additional $13.4 \mu\text{s}$ after the cooling light was turned off, in order to prepare the initial state $|i\rangle$. Our vacuum cell was magnetically shielded by a three-fold permalloy and the residual magnetic field was about $100 \mu\text{G}$. In the measurement period, the *write* and *read* pulses illuminated the atomic ensemble with a repetition cycle of $1 \mu\text{s}$. Each cycle finished with illumination of 200 ns long repumping pulse to initialize the atomic ensemble. The *write* and *read* pulses were produced by external cavity laser diodes (ECLDs), and their spatial modes were purified by passing through SMF1 and SMF3, respectively. A 100 ns long *write* pulse having 250 nW peak intensity was focused into the atomic ensemble with a Gaussian beam waist of $400 \mu\text{m}$, where the detuning of the *write* pulse was set to -10 MHz . Anti-Stokes photons were coupled to a single mode fiber (SMF2) after being diffracted by the computer generated hologram (H1). The coupling efficiency to SMF2 was maximized for the LG_{00} mode having a beam waist of $140 \mu\text{m}$ at the center of the atomic ensemble. We utilized a reflection-type phase hologram blazed to increase the diffraction efficiency up to 45% . Two types of holograms were used in the experiment, one having no dislocation and the other having a single dislocation located at its center. Our experiment using classical light demonstrated that the combination of a hologram and a single mode fiber could achieve mode detection with a distinction ratio of approximately $1000 : 1$ between LG_{00} and LG_{01} modes.

After the writing process, a 100 ns long *read* pulse having a $150 \mu\text{W}$ peak intensity was irradiated to the atomic ensemble. In all of the experiments the variable delay time δt was set to 100 ns . Stokes photons were collected by SMF4 using an optical system similar to that used for anti-Stokes photons.

Two single mode fibers (SMF1, SMF3) were aligned so that the *write* and the *read* pulses

counter-propagating along the z axis shared the same single spatial mode. Similarly, anti-Stokes and Stokes photons counter-propagating along the z' axis shared a single spatial mode when the corresponding mode conversions were chosen for the holograms. The crossing angle between the z and z' axes was set to about 2.5° in order to spatially separate the weak anti-Stokes (Stokes) photons from the strong *write (read)* pulses (14).

The anti-Stokes and Stokes photons coupled into SMF2 and SMF4 were directed onto silicon avalanche photodiodes D1 and D2 (Perkin-Elmer model SPCM-AQR-14; detection efficiency, 0.62) for photon counting. The outputs of D1 and D2 were fed to the start and the stop inputs of the time interval analyzer (TIA). Fig.2-A shows the experimental results for the time-resolved coincidence over 1000 s between the anti-Stokes photons and Stokes photons of LG_{00} mode, from which the normalized cross intensity correlation function was estimated to be $g_{AS,S}(0) = 22.2 \pm 2.9$. The repetition rate of our experiment was $4.5 \times 10^5 \text{ s}^{-1}$. The count rate for the anti-Stokes photons was $3.1 \times 10^2 \text{ s}^{-1}$ and the coincidence count rate was 2.0 s^{-1} . The measured transmission efficiency from the atomic ensemble to the detector was about 0.17. The excitation probability is estimated to be about 6.6×10^{-3} , which confirms that the detected photons were well approximated by the single photon state.

In order to evaluate the entanglement of OAM states, we investigated the coincidence counts under the various measurement bases. Here we utilize the following notation: $|+\rangle \equiv (|0\rangle + |1\rangle)/\sqrt{2}$, $|-\rangle \equiv (|0\rangle - |1\rangle)/\sqrt{2}$, $|u\rangle \equiv (|0\rangle + i|1\rangle)/\sqrt{2}$ and $|d\rangle \equiv (|0\rangle - i|1\rangle)/\sqrt{2}$. Figs.2-B, C, and D graphically show the coincidence counts between anti-Stokes photons and Stokes photons, where the measurement was performed for four possible combinations of the three sets of orthogonal states $\{|0\rangle, |1\rangle\}$, $\{|+\rangle, |-\rangle\}$, and $\{|u\rangle, |d\rangle\}$. In the experiment, drifting of the optical alignment was inevitable due to the complexity of the system and each measurement was thus performed over a relatively short duration (100 s). Fig.2-B clearly shows correlation of OAM between anti-Stokes and Stokes photons arising from angular momentum conservation

law. Note that such a correlation can be obtained even in the case of a simple mixture of $|0\rangle_{AS}|0\rangle_S$ and $|1\rangle_{AS}|1\rangle_S$ states. The characteristics of entanglement can be found from Figs.2-C and D, where strong correlation was observed on the basis with superposition states. In order to verify whether the system was really entangled or not, we calculated a lower bound of the fidelity to the maximally entangled state $(|0\rangle_{AS}|0\rangle_S + |1\rangle_{AS}|1\rangle_S)/\sqrt{2}$ from the coincidences determined from Fig.2-C and D (15). The lower bound is given by $p + q - 1$, where p (q) is the diagonal fraction in Fig.2-C(D), and is calculated as $0.70 \pm 0.08 > 0.5$. This confirms entanglement between anti-Stokes and Stokes photons. From these results, entanglement of the OAM states between anti-Stokes photon and the atomic ensemble was verified.

For the determination of the full state of the atoms and the anti-Stokes photon, we performed two-qubit state tomography (16, 17), where the density matrix was reconstructed from the experimentally obtained coincidences for various combinations of the measurement basis. A graphical representation of the reconstructed density matrix is shown in Fig.3. From the density matrix, the entanglement of formation (EOF) and the purity are estimated to be 0.76 ± 0.17 and 0.92, respectively. The EOF obtained was relatively small compared with typical values for the pair of photons generated by the PDC process (17). As is clear from Fig.2-B, the dominant factor limiting EOF is the difference in the relative amplitude between $|0\rangle_{AS}|0\rangle_S$ and $|1\rangle_{AS}|1\rangle_S$, in other words, $|0\rangle_{AS}|0\rangle_a$ and $|1\rangle_{AS}|1\rangle_a$. Since the relative amplitude is considered to be dependent on the waist size of the *write* pulse (12), it should be possible to increase EOF by optimizing the focusing of the beam.

In summary, we demonstrated entanglement of OAM states between a collective atomic excitation and a photon. Storage of a quantum state involving the spatial mode associated with electromagnetically induced transparency (18) will enable us to share the higher-dimensional entanglement between two remote atoms. Since, in principle, the quantum mechanical phase of atoms can be manipulated by applying a far off resonant laser beam, entanglement concentration

(5) in an atomic ensemble could also be achieved. The experiment described in this paper raises the possibility that the atomic ensemble could be projected to any desired OAM state through the measurement of an anti-Stokes photon. By using a Bose-Einstein condensate as an atomic ensemble, any desired yrast states (19) could be generated in the range of $-N\hbar$ to $N\hbar$.

We gratefully acknowledge M. Ueda, K. Usami, K. Akiba and A. Wada for their valuable comments and stimulating discussions. We also thank T. Yonemura, K. Bito and M. Moriya for supplying computer generated holograms. This work was supported by Grant-in-Aid for Young Scientists (A), and the 21st Century COE Program at Tokyo Tech “Nanometer-Scale Quantum Physics” by the MEXT.

References and Notes

1. M. Bourennane, A. Karlsson, G. Björk, *Phys. Rev. A* **64**, 012306 (2001).
2. H. Bechmann-Pasquinucci, A. Peres, *Phys. Rev. Lett.* **85**, 3313 (2000).
3. G. F. Calvo, A. Picon, E. Bagan, *Phys. Rev. A* **73**, 013805 (2006).
4. A. Mair, A. Vaziri, G. Weihs, A. Zeilinger, *Nature* **412**, 313 (2001).
5. A. Vaziri, J.-W. Pan, T. Jennewein, G. Weihs, A. Zeilinger, *Phys. Rev. Lett.* **91**, 227902 (2003).
6. N. K. Langford, *et al.*, *Phys. Rev. Lett.* **93**, 053601 (2004).
7. D. N. Matsukevich, *et al.*, *Phys. Rev. Lett.* **95**, 040405 (2005).
8. L.-M. Duan, M. D. Lukin, J. I. Cirac, P. Zoller, *Nature* **414**, 413 (2001).
9. C. W. Chou, *et al.*, *Nature* **438**, 828 (2005).

10. D. N. Matsukevich, *et al.*, *Phys. Rev. Lett.* **96**, 030405 (2006).
11. A. Vaziri, G. Weihs, A. Zeilinger, *J. Opt. B: Quantum Semiclass. Opt.* **4**, S47 (2002).
12. J. P. Torres, A. Alexandrescu, L. Torner, *Phys. Rev. Lett.* **68**, 050301 (2003).
13. M. Fleischhauer, M. D. Lukin, *Phys. Rev. A* **65**, 022314 (2002).
14. V. Balić, D. A. Braje, P. Kolchin, G. Yin, S. E. Harris, *Phys. Rev. Lett.* **94**, 183601 (2005).
15. K. Nagata, M. Koashi, N. Imoto, *Phys. Rev. A* **65**, 042314 (2002).
16. K. Usami, Y. Nambu, Y. Tsuda, K. Matsumoto, K. Nakamura, *Phys. Rev. A* **68**, 022314 (2000).
17. D. F. V. James, P. G. Kwiat, W. J. Munro, A. G. White, *Phys. Rev. A* **64**, 052312 (2001).
18. T. Chanelière, *et al.*, *Nature* **438**, 833 (2005).
19. B. Mottelson, *Phys. Rev. Lett.* **83**, 2695 (1999).

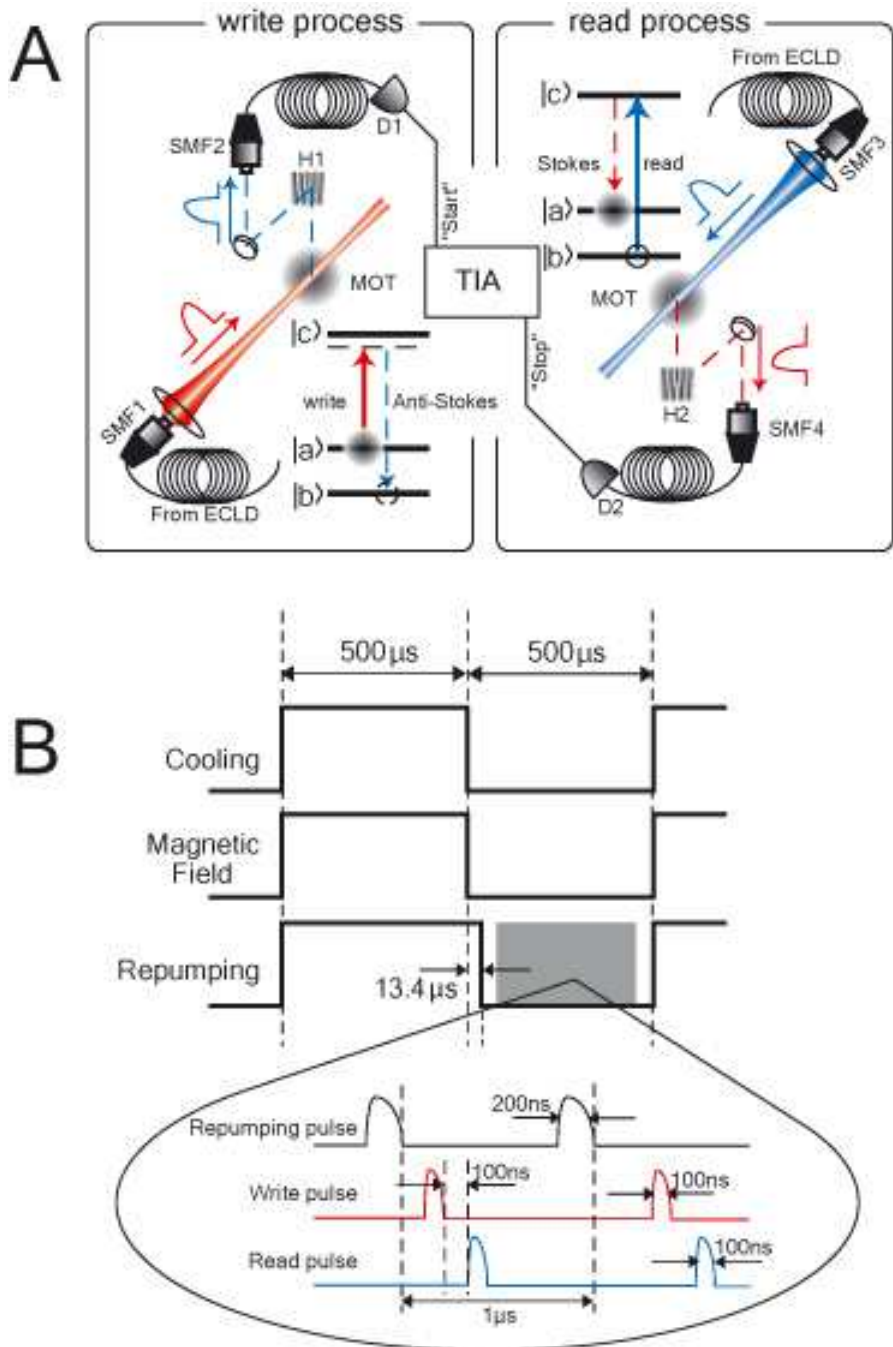


Figure 1: A, Schematic of experimental setup. *Write* and *read* pulses propagate into a cloud of cold ^{87}Rb atoms (MOT), and generate the correlated output pair of anti-Stokes and Stokes photons. SMF1, 2, 3, and 4, single mode fibers; H1 and H2, computer generated holograms; D1 and D2, detectors; TIA, time interval analyzer. B, Depicts the timing sequence for data acquisition.

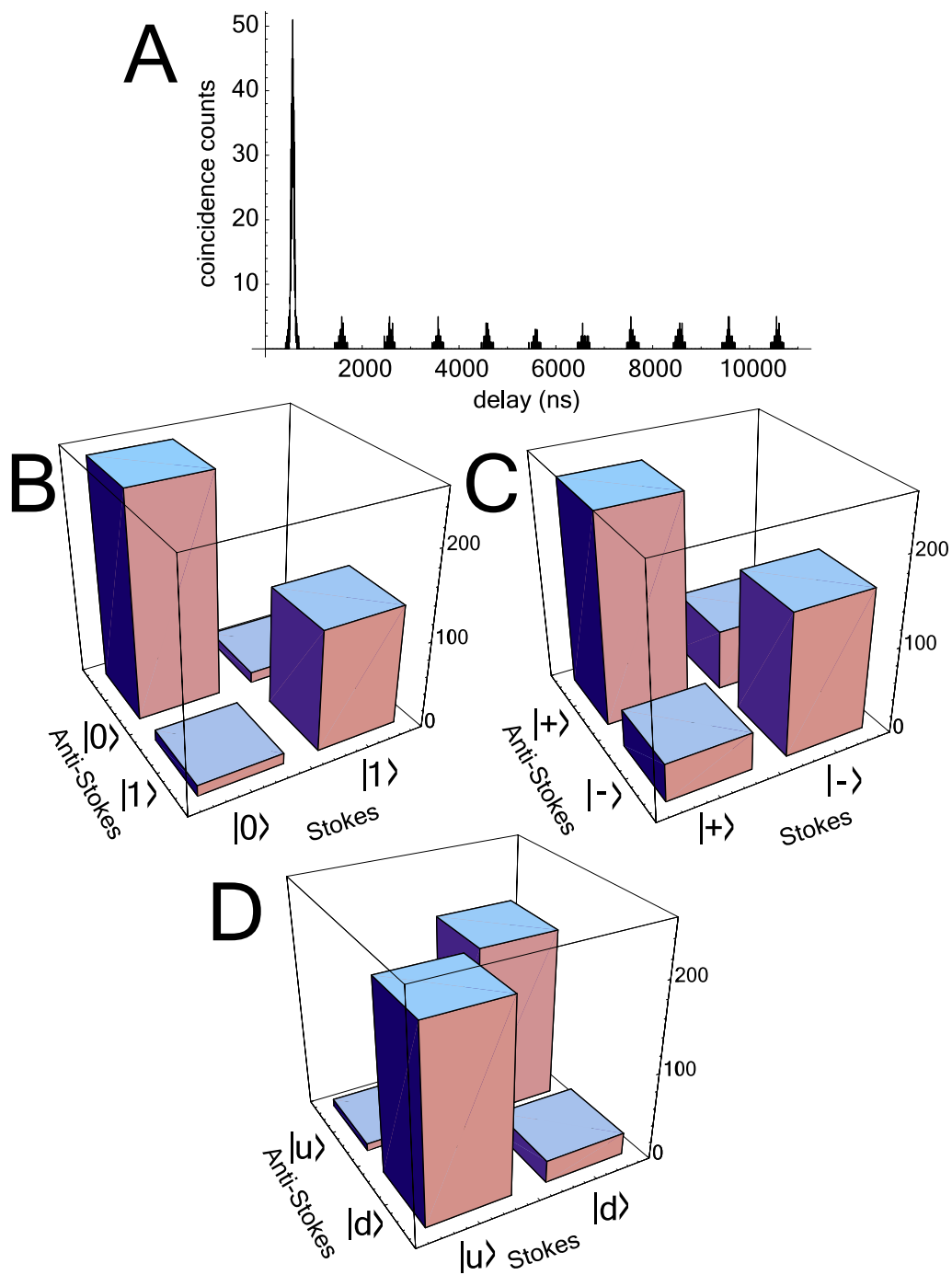
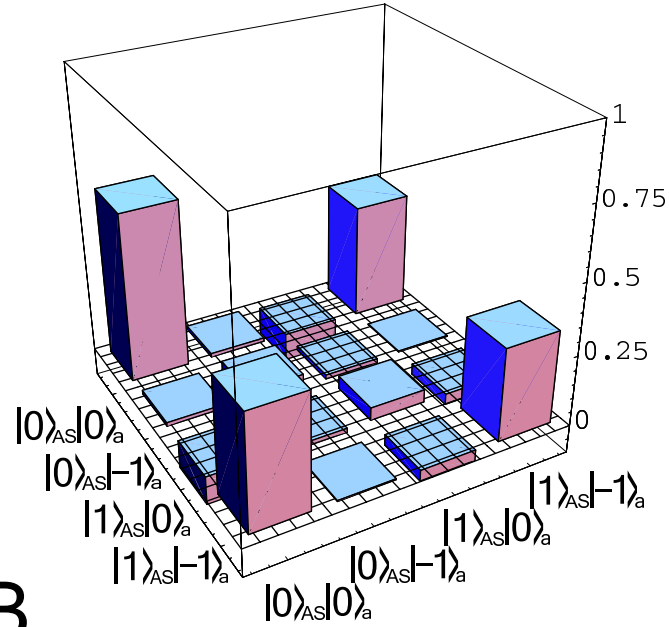


Figure 2: A, Time-resolved coincidence counts, where the time resolution was set to 1.6 ns. B, C and D are the coincidences in the various measurement basis.

A



B

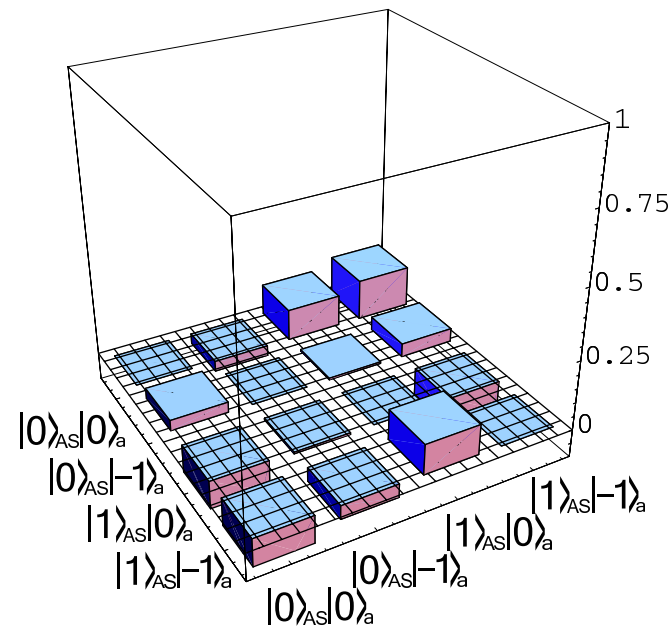


Figure 3: Graphical representation of the reconstructed density matrix. A is the real part and B is the imaginary part.